

# Space Shuttle Entry Guidance Performance Results

Jon C. Harpold\*

NASA Johnson Space Center, Houston, Texas

and

Donald E. Gavert†

Rockwell International, Downey, California

The performance of the Orbiter entry guidance system has been excellent during all of the space shuttle flights. This paper summarizes the entry guidance objectives and control concepts, reviews the entry guidance preflight predicted results, and presents the significant entry guidance and trajectory flight results from the first three Orbiter flights. Emphasis is on the steady-state characteristics from the first and third missions and on the transitory response characteristics resulting from the major Orbiter aerodynamic test maneuvers on the second flight.

## Nomenclature

$C_D$	= aerodynamic drag coefficient
$D$	= drag deceleration
$D_{REF}$	= desired drag deceleration
$f_1$	= roll controller gain on drag deceleration error
$f_2$	= roll controller gain on altitude rate error
$f_3$	= roll controller gain on drag deceleration integral feedback term
$f_4$	= roll controller gain on angle-of-attack error
$f_5$	= angle-of-attack controller gain on drag deceleration error
$\dot{H}$	= navigation derived altitude rate
$\dot{H}_{REF}$	= desired altitude rate
$L/D$	= Orbiter lift-to-drag ratio
$L/D_{REF}$	= reference lift-to-drag ratio
$\alpha$	= angle of attack
$\alpha_{CMD}$	= angle-of-attack command
$\alpha_{SCHEDULE}$	= desired nominal angle-of-attack profile
$\phi_{CMD}$	= roll angle command

## Introduction

THE Orbiter entry guidance system controls the Space Shuttle Orbiter to the desired landing site between the initial atmospheric penetration point and an Earth-relative velocity of 2500 ft/s. At 2500 ft/s, control of the Orbiter is transferred to the terminal area energy management (TAEM) system. During entry, the Orbiter has traveled from an initial range-to-landing site of approximately 4400 n. mi. to a range-to-landing site of approximately 60 n. mi. at the TAEM interface.

## Orbiter Entry Guidance Concept

The entry guidance system is based on the concept that the range to be flown during entry is a unique function of the drag deceleration profile flown throughout the entry. The range prediction during entry is based on analytic equations that are simple drag deceleration functions of Earth-relative velocity above Mach 10.5 and energy with respect to the Earth below

Mach 10.5. Flight through the entry corridor is accomplished by linking these simple drag deceleration functions together in series in order to define a drag deceleration reference profile.

The desired drag deceleration profile shape is designed by input constants in the flight software. Figure 1 presents a typical drag deceleration profile that consists of five drag deceleration segments. The number of segments and the shape of each segment was selected based on the nature of the predominant vehicle constraint during the corresponding velocity range. Figure 1 also presents the entry corridor and the predominant constraints.

During entry, the level of the drag deceleration profile is adjusted such that the analytically predicted range and the range to the target as computed by the navigation system are equal. In addition to the drag deceleration profile, the altitude rate and the component of  $L/D$  in the vertical plane formed by the position and Earth-relative velocity vectors associated with the drag deceleration profile are also computed.

With the determination of the desired drag deceleration profile, a controller law was developed to compute vehicle attitude commands to control the Orbiter to the desired drag deceleration profile. The control law response to drag profile deviations is represented by a second-order differential equation with constant coefficients. The control law is

$$(L/D)_{CMD} = (L/D)_{REF} + f_1(D - D_{REF}) + f_2(\dot{H} - \dot{H}_{REF}) + f_3\{D - D_{REF}\} \quad (1)$$

The last term of this controller equation prevents steady-state trajectory deviations caused by inaccuracies in the navigation computation of the altitude rate. The commanded  $L/D$  can be achieved by either controlling the Orbiter angle of attack or the roll angle, or a combination of both control parameters. The Orbiter guidance system uses a combination of roll angle and angle-of-attack modulation for trajectory control.

Roll angle was chosen as the primary trajectory control variable so that the angle-of-attack profile could be selected to minimize the aerodynamic heating environment while achieving the required cross-range capability. The magnitude of the roll angle controls the Orbiter to the desired drag deceleration profile and the direction of the roll angle controls the cross-range of the Orbiter through a series of roll reversals. The roll angle command equation is

$$\phi_{CMD} = \cos^{-1}[(L/D)_{CMD}/L/D] + f_4(\alpha - \alpha_{SCHEDULE}) \quad (2)$$

Because the trajectory response to roll angle modulation is relatively slow, the angle of attack is modulated over a small

Presented as Paper 82-1600 at the AIAA Guidance and Control, Atmospheric Flight Mechanics, and Astrodynamics Conference, San Diego, Calif., Aug. 9-11, 1982; submitted Aug. 9, 1982; revision received April 8, 1983. This paper is declared a work of the U.S. Government and therefore is in the public domain.

\*Chief, Descent Flight Analysis Branch.

†Supervisory Engineer, Entry Systems and Flight Operations.

angle-of-attack corridor to achieve the desired drag acceleration profile on a short-period basis. The roll angle command is compensated to control the angle of attack back to the desired schedule on a longer period basis. This function is accomplished through the last term in the roll angle command Eq. (2). The angle-of-attack modulation capability was added to the guidance control law to provide additional trajectory control during roll reversals and to compensate for short-period disturbances such as atmospheric density gradients. The angle-of-attack command equation is simply

$$\alpha_{CMD} = \alpha + C_D (D_{REF} - D) / f_5 \quad (3)$$

Figure 2 presents a comparison of the angle-of-attack and roll angle performance during entry and shows the response of the angle-of-attack channel to the roll angle reversals. A complete discussion of the guidance system concept and the equations can be found in Ref. 1.

### Preflight Test Procedures

Entry guidance, like most other Shuttle guidance, navigation, and control (GN&C) systems, has been tested through basically a two-stage process. The initial stage involves almost exclusively nonreal-time mathematical model simulations focusing on inherent design requirements and capabilities. This includes both nominal and stress testing that attempts to define the operating limits for the system under investigation. For entry guidance, the testing has concentrated on ranging solution, controller law stability, transient response, and sensitivity to system errors (i.e., navigation state errors) and/or dispersions (i.e., off-nominal aerodynamics, winds, etc.). The results of this phase of testing are then used to define an optimal trajectory profile for achieving the desired goals while maintaining system/vehicle constraints under the full range of potential conditions that might be encountered.

The second phase of testing for the Shuttle GN&C involves primarily formal verification testing utilizing the actual Shuttle avionics elements (i.e., flight software, flight computer hardware, cockpit configurations, etc.). These elements are linked to external analog/digital modeling functions to provide an extremely realistic "real-time" evaluation of flight operations and vehicle performance. This total system's test and verification capability enables thorough assessment not only of the GN&C "as-built" performance but also of the critical "man/machine" interface and resultant interactions not possible with nonreal-time mathematical model situations.

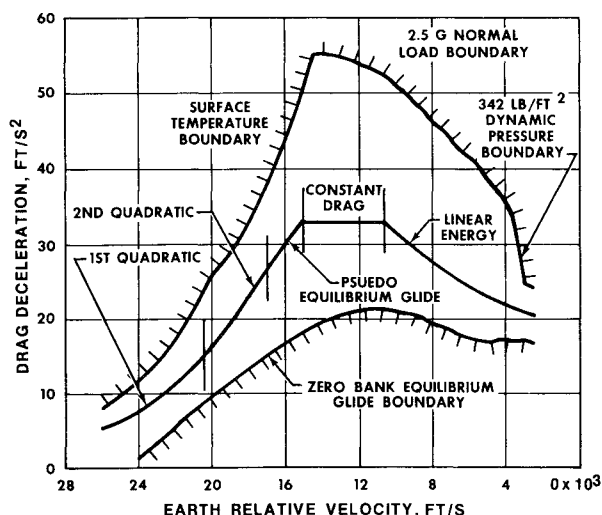


Fig. 1 Entry corridor.

For entry guidance, the preceding overview of the testing process is directly applicable. Extensive use of nonreal-time simulations has been used as the major element in defining the functional guidance design requirements, as currently established, as well as the performance capability envelopes. The final flight software/avionics and performance verification involves two simulation entities: the IBM Software Development Laboratory (SDL), used primarily for verification of flight software functions and some limited performance testing; and the Rockwell International (RI) Flight Simulation Laboratory (FSL), used to verify the overall functional and performance operations of the avionics and integrated GN&C in a real-time man-in-the-loop environment.

The crucial role played by nonreal-time or off-line simulations becomes obvious with the knowledge that a

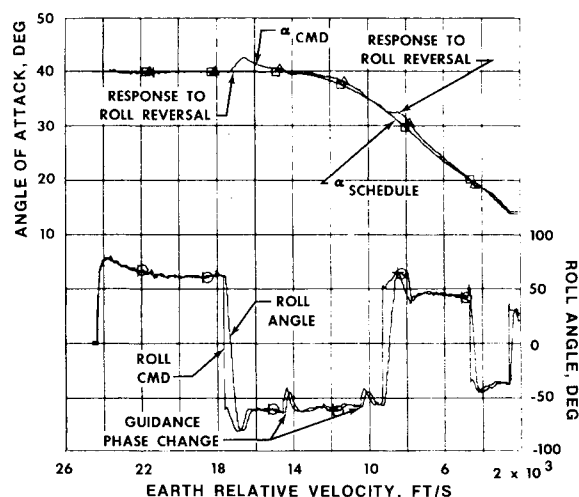


Fig. 2 Angle-of-attack and roll angle performance.

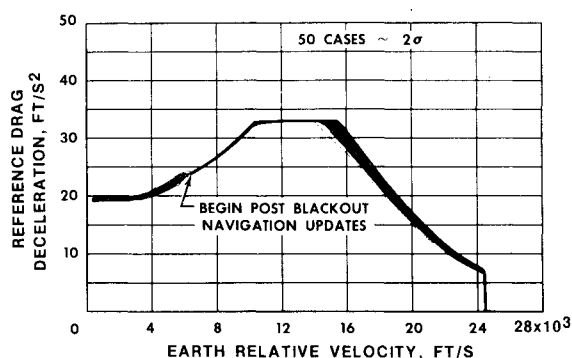


Fig. 3 Drag reference profiles from Monte Carlo analysis.

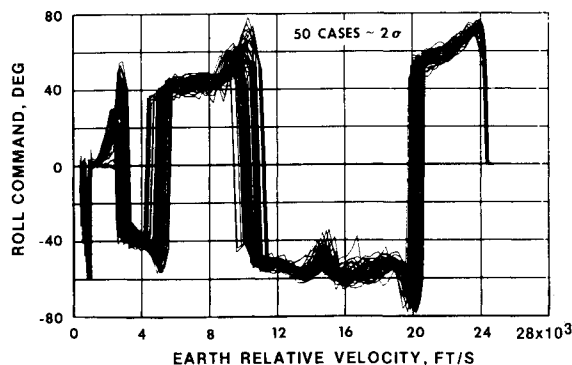


Fig. 4 Roll command profiles from Monte Carlo analysis.

predefinition for the flight software configuration is a sufficient and necessary condition to its building, testing, and verification. After defining the guidance concept, the emphasis for off-line simulations centered on establishing and verifying the trajectory-shaping constants used by the guidance that would satisfy both performance and flight test objectives. Notable constraints or requirements imposed on the guidance-shaping constants were satisfaction of thermal protection system (TPS) test objectives, aerodynamic/flight control system lateral stability restrictions, fundamental ranging requirements, and acceptable entry/TAEM interface conditions.

Once the basic nominal trajectory is defined and appropriate shaping constraints established, the next phase of testing (utilizing off-line simulations) involves establishing a capability envelope for accommodating off-nominal conditions. This process not only establishes the acceptable operating range for the guidance but also determines the sensitivity of the guidance to various dispersions whether "environmental" (i.e., winds, atmospheric, aerodynamic, etc.) or GN&C system-related [i.e., navigation errors, flight control system (FCS) tolerances, etc.]. These sensitivities are then used to establish "worst-case" conditions to be used later in the integrated GN&C performance verification performed at FSL.

Off-line "deterministic" stress testing tends to be accomplished in two degrees of severity. The less severe method relies on sensitivity factors for guidance performance as established through simulations examining the effects of single dispersion sources. This "one-by-one" dispersion effect process ultimately results in a total set of root sum square (rss) derived sensitivity factors for all the individual dispersion sources, such that the net effect is an ability to model  $1\sigma$ ,  $2\sigma$ , or  $3\sigma$  dispersed trajectories. The more severe stress testing approach applies "worst-case" (i.e.,  $3\sigma$ ) dispersions to all the trajectory and guidance sensitive parameters to establish "worst-on-worst" (w-o-w) operating limits. Off-line simulation w-o-w studies rely on the rss sensitivity factors to establish the conditions necessary to best configure the stress test for the particular performance element under investigation. These w-o-w off-line tests further help to establish the FSL test configurations and expected performance results.

The other type of off-nominal entry guidance testing available through off-line simulations is a Monte Carlo analysis. In these case studies, potential dispersion sources, whether environmental or systems related, are randomly sampled for each individual member of the test case series. Both additive and compensating combinations for the dispersions can occur. The net result, given a 50 or 100 case sampling, is an overall estimated  $3\sigma$  guided trajectory envelope. The derived probability envelopes for critical trajectory parameters provide an excellent means for pinpointing potential problem areas for not only the guidance but also other GN&C subsystems. A useful result of Monte Carlo analysis is the ability to predict the  $1\sigma$ ,  $2\sigma$ ,  $3\sigma$  envelopes for key guidance-related events such as roll reversals, phase transitions, entry/TAEM interface conditions, etc. This is crucial to flight planning with regard to scheduling descent flight test objectives such as the aerodynamics/FCS maneuvers so that interference with critical guidance-related events can be avoided. An example of the Monte Carlo output can be seen in Figs. 3-5. These figures show the expected

performance bandwidths for the drag deceleration, roll angle command, and the angle-of-attack profile for the STS-3 mission.

As mentioned previously, the primary tests related to the verification of the actual mechanization of guidance functional requirements are preformed at IBM's SDL. These tests involve functional checks at the module level (i.e., guidance, navigation, etc.) as well as integrated GN&C nominal and stress performance cases. The SDL tests provide a means for validating the flight software configuration through comparisons with similarly configured off-line simulations. By reviewing SDL test data against other simulations, potential mechanization discrepancies can be uncovered and investigated early in the software development cycle and, if warranted, be corrected without jeopardizing the critical scheduling of delivered flight software releases.

The final flight performance verification of entry guidance as well as all other descent GN&C functions for both the primary and backup flight system are achieved through extensive testing at RI's FSL. It is at FSL where the total integrated GN&C system is exercised in a real-time man-in-the-loop environment using actual Shuttle avionics elements. The FSL facility maintains an extremely sophisticated and complex spectrum of mathematical model capabilities so that

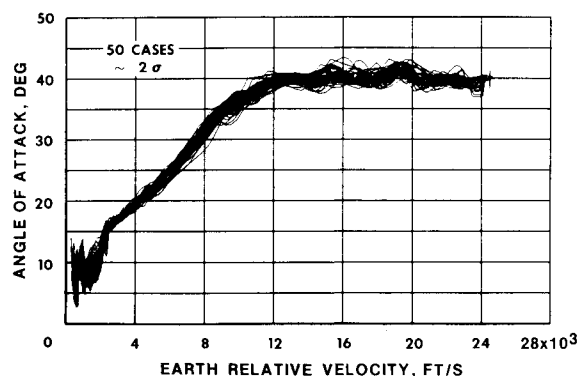


Fig. 5 Angle-of-attack profiles from Monte Carlo analysis.

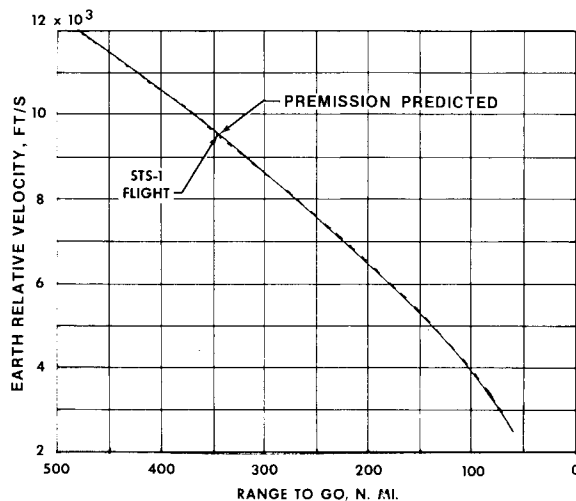


Fig. 6 STS-1 velocity range data.

Table 1 Summary of entry conditions for STS-1, STS-2, and STS-3

Mission	Entry date	Landing site	Entry range, n. mi.	Range at TAEM interface, n.mi.	Maximum normal load factor, g	Maximum dynamic pressure, lb/ft <sup>2</sup>
STS-1	April 14, 1981	Edwards AFB, Calif.	4372	58.9	1.60	217
STS-2	Nov. 14, 1981	Edwards AFB, Calif.	4443	59.7	1.61	215
STS-3	March 30, 1982	White Sands, N. Mex.	4136	59.1	1.62	220

all factors having an effect on descent performance can be accurately represented.

The total entry guidance capability verification is achieved through a series of w-o-w performance stress cases as defined through prior offline simulation experience. Both automatic and manual control modes are exercised to assess guidance operations for either of these configurations under stress conditions. Not only trajectory performance but also guidance compatibility with related functions such as crew displays are thoroughly assessed. Potential problems occurring from stress tests are evaluated throughout the descent GN&C community. Resolution of concerns may entail alterations to crew procedures and potentially even changes to the flight software if necessary to minimize flight risk. When successfully completed the FSL testing then becomes the major factor in certifying the flight readiness of entry guidance as well as the total Shuttle descent GN&C. The end result of all preflight testing for STS-1, STS-2, and STS-3 showed no anticipated problem areas and significant margin in guidance performance.

### Flight Results

The flight test performance of the entry guidance system on the first three Space Shuttle missions has been excellent. No guidance flight anomalies or unexpected performance characteristics occurred on these missions. The first mission (STS-1) was flown primarily in the automatic control mode except for a 1 min interval at an Earth-relative velocity of

4700 ft/s during the third planned roll reversal. The second switch to manual control occurred just prior to entry/TAEM interface at an Earth-relative velocity of 2500 ft/s. Both these manual control periods were planned premission.

During the second mission (STS-2), 24 aerodynamic test maneuvers were performed to better define the Orbiter aerodynamic characteristics. Nine of these maneuvers were performed in the pitch axis, 14 in the roll/yaw axis, and one speedbrake sweep was performed during the landing phase. All these test maneuvers were flown in the manual control mode. In addition, of the four planned entry roll reversals, three were executed in the automatic mode and one was executed in the manual control mode. A total of 52 control mode switches was performed during entry on the second flight. Thus, this flight was an excellent test of the control mode capabilities and guidance system stability and convergence characteristics.

The third mission (STS-3) was again flown mostly in the automatic control mode during entry. However, five aerodynamic test maneuvers and the initial guidance-commanded roll maneuver at Mach 24 were flown in the manual control mode. Table 1 presents a summary of the entry conditions for these missions.

Figure 6 presents the range-to-go/Earth-relative velocity data for the latter part of the entry (12,000-2500 ft/s) on the STS-1 mission. Figure 6 shows that the entry guidance system controlled the entry trajectory on the exact path predicted preflight. Figures 7 and 8 present the range-to-go/Earth-relative velocity data for the STS-2 and STS-3 missions. Again, even with the extensive aerodynamic test maneuvers on STS-2, the entry guidance was able to control the trajectories to the predicted preflight nominals.

As mentioned earlier, the entry guidance system controls the entry trajectory by controlling the drag deceleration profile

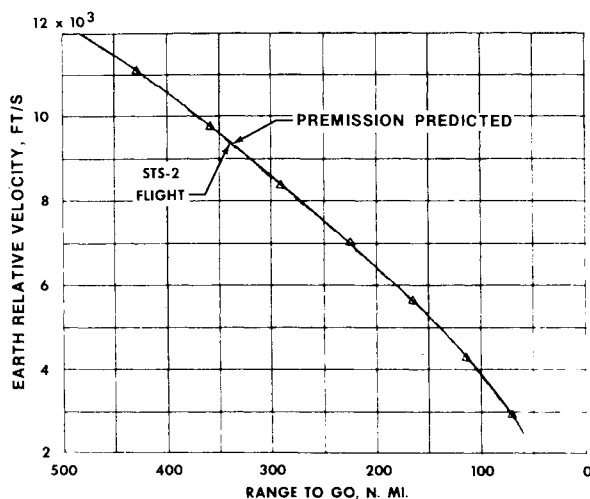


Fig. 7 STS-2 velocity range data.

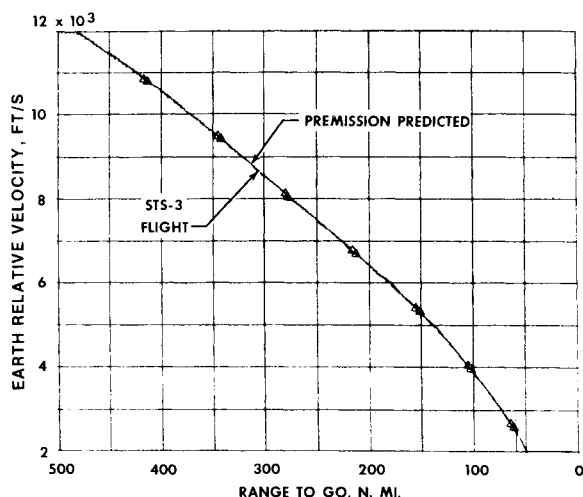


Fig. 8 STS-3 velocity range data.

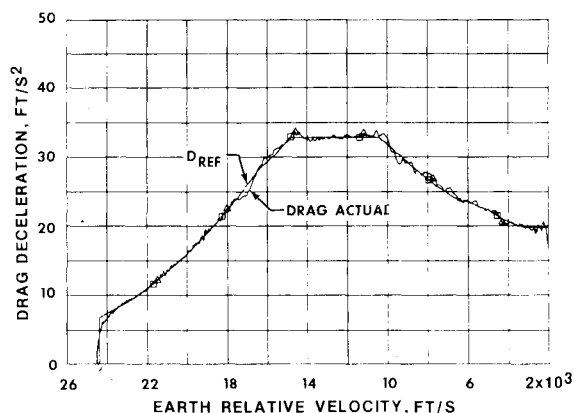


Fig. 9 STS-3 drag profile data.

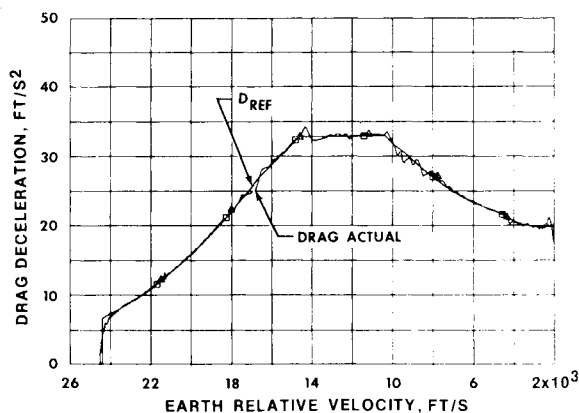


Fig. 10 Premission estimate of drag profile.

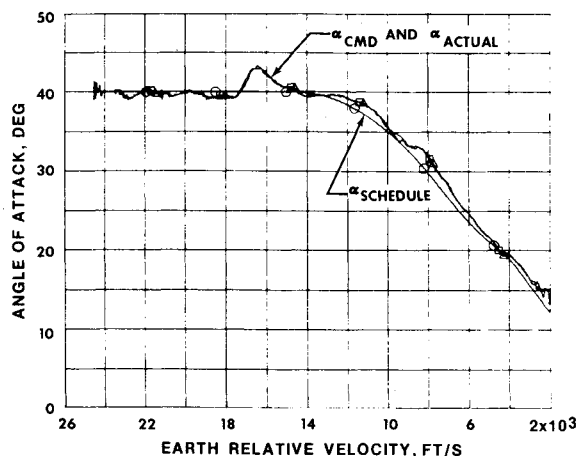


Fig. 11 STS-3 angle-of-attack profile.

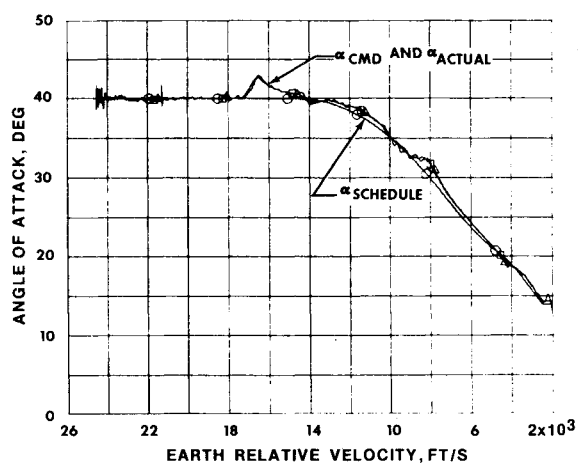


Fig. 12 Prepermission estimate of angle-of-attack profile.

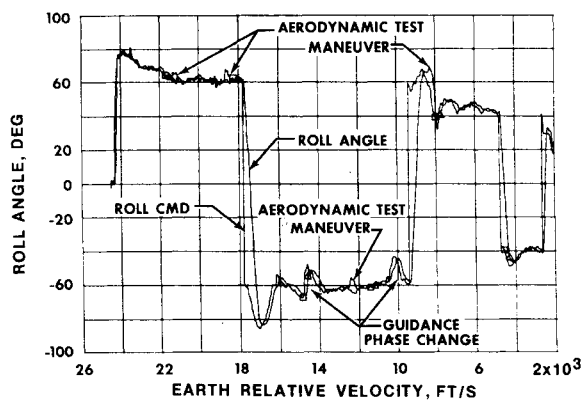


Fig. 13 STS-3 roll angle profile.

of the Orbiter to the desired drag reference profile, which is adjusted to compensate for ranging errors. Figure 9 presents the STS-3 drag profile data and Fig. 10 the corresponding drag profile data from the premission estimated profile.

A comparison of these profiles shows an almost exact match between the flight data and the premission estimated data. Similar profile comparison results occurred on the first two flights. Figure 11 presents the STS-3 angle-of-attack profile and Fig. 12 the premission estimated data.

A comparison of these data indicated that the angle-of-attack channel performed as predicted and that slightly larger angle-of-attack changes were required by the entry guidance

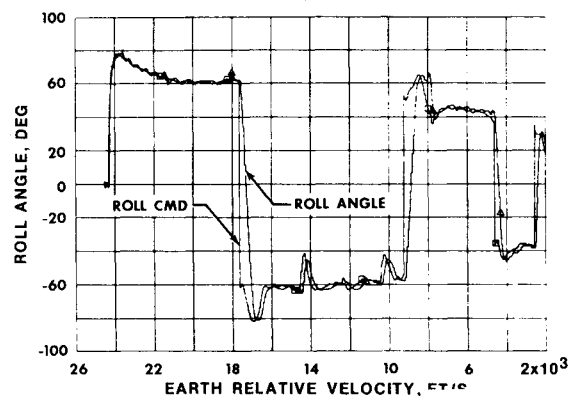


Fig. 14 Prepermission estimate of roll angle profile.

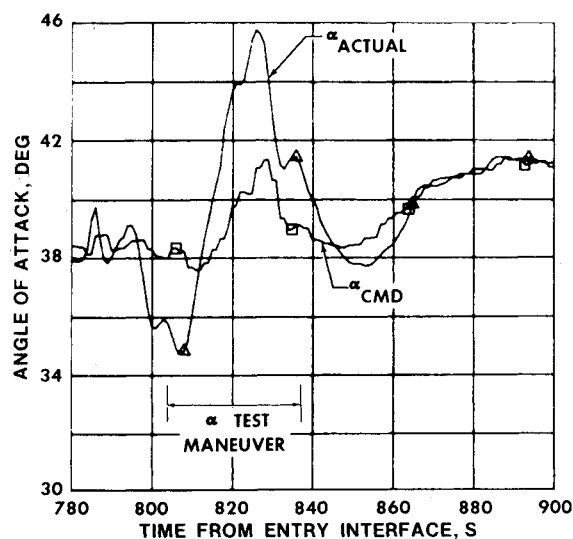


Fig. 15 Angle of attack command response to angle-of-attack maneuver on STS-2.

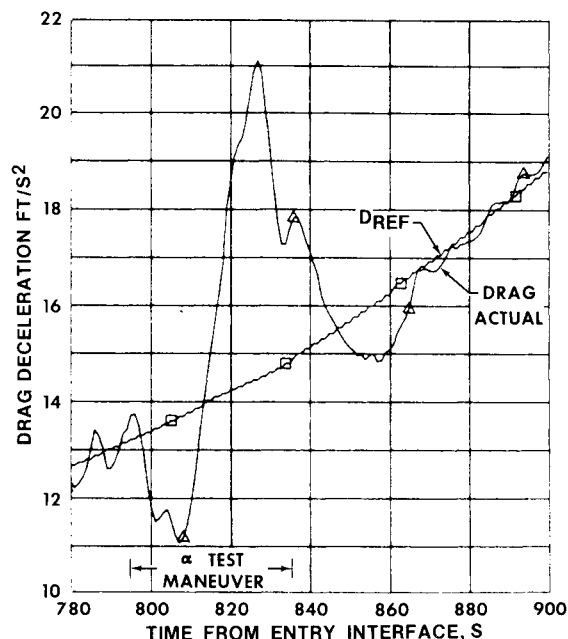


Fig. 16 Guidance trajectory control response to angle-of-attack test maneuver on STS-2.

system to compensate the drag profile deviations during the planned roll reversals. Also of interest are the smaller angle-of-attack changes between 17,000 and 23,000 ft/s. The slight lowering of the angle-of-attack profile for short time periods is characteristic of the effect of atmospheric density gradients on the Orbiter trajectory and guidance.

The roll channel performance can be seen in Fig. 13 (STS-3 flight data) and Fig. 14 (premission estimate). A comparison of these data shows that each roll reversal for cross-range control occurred at almost the exact velocity as predicted premission. This is a direct indication that the lift-to-drag ratio of the Orbiter was near nominal magnitude. Also note that the regular deadbanding effect of the flight control system roll channel in the predicted data is not clearly as evident in the STS-3 flight data. This lack of deadbanding is probably due to the pitch and roll axes responding to atmospheric and wind shear effects, which prevented the system from establishing a steady-state deadbanding effect. However, reaction control system (RCS) usage during this time period does not indicate that these effects resulted in increased RCS usage over the magnitude estimated premission.

As mentioned earlier, the STS-2 mission demonstrated the ability of the entry guidance system to compensate for

transient effects caused by the aerodynamic test maneuvers. Figures 15 and 16 show the response of the guidance system to the large angle-of-attack pushover and pullup test maneuvers and the resultant Orbiter response in the drag deceleration plane.

These plots show that the guidance system had no difficulty in reconverging the Orbiter drag deceleration profile back to the desired reference profile after the large angle-of-attack test maneuver.

### Conclusion

The results of the first three Space Shuttle missions have not only verified the entry guidance concept but have also demonstrated the stability of the guidance system and the validity of the premission planning and verification program. The final flight test completed the certification process and demonstrated the operational readiness of the entry guidance system.

### Reference

- <sup>1</sup>Harpold, Jon C. and Graves, Claude A. Jr., "Shuttle Entry Guidance," *Journal of the Aeronautical Sciences*, Vol. XXVII, No. 3, July-Sept. 1979.

---

## *From the AIAA Progress in Astronautics and Aeronautics Series*

# **SPACE SYSTEMS AND THEIR INTERACTIONS WITH EARTH'S SPACE ENVIRONMENT—v. 71**

*Edited by Henry B. Garrett and Charles P. Pike, Air Force Geophysics Laboratory*

This volume presents a wide-ranging scientific examination of the many aspects of the interaction between space systems and the space environment, a subject of growing importance in view of the ever more complicated missions to be performed in space and in view of the ever growing intricacy of spacecraft systems. Among the many fascinating topics are such matters as: the changes in the upper atmosphere, in the ionosphere, in the plasmasphere, and in the magnetosphere, due to vapor or gas releases from large space vehicles; electrical charging of the spacecraft by action of solar radiation and by interaction with the ionosphere, and the subsequent effects of such accumulation; the effects of microwave beams on the ionosphere, including not only radiative heating but also electric breakdown of the surrounding gas; the creation of ionosphere "holes" and wakes by rapidly moving spacecraft; the occurrence of arcs and the effects of such arcing in orbital spacecraft; the effects on space systems of the radiation environment, etc. Included are discussions of the details of the space environment itself, e.g., the characteristics of the upper atmosphere and of the outer atmosphere at great distances from the Earth; and the diverse physical radiations prevalent in outer space, especially in Earth's magnetosphere. A subject as diverse as this necessarily is an interdisciplinary one. It is therefore expected that this volume, based mainly on invited papers, will prove of value.

737 pp., 6 × 9, illus., \$30.00 Mem., \$55.00 List

TO ORDER WRITE: Publications Dept., AIAA, 1290 Avenue of the Americas, New York, N.Y. 10104